Anatomy of the ρ resonance from lattice QCD at the physical point *

Wei Sun(孙玮)[1,2] Andrei Alexandru[3] Ying Chen(陈莹)[1,2;1)] Terrence Draper[4]
Zhaofeng Liu(刘朝峰)[1,2] Yi-Bo Yang(杨一玻)[5]
(χQCD Collaboration)

[1] Institute of High Energy Physics, Chinese Academy of Sciences, Beijing 100049, China
[2] School of Physics, University of Chinese Academy of Sciences, Beijing 100049, China
[3] Department of Physics, George Washington University, Washington, DC 20052, USA
[4] Department of Physics and Astronomy, University of Kentucky, Lexington, KY 40506, USA
[5] Department of Physics and Astronomy, Michigan State University, East Lansing, MI 48824, USA

Abstract: We propose a strategy to access the $q\bar{q}$ component of the ρ resonance in lattice QCD. Through a mixed action formalism (overlap valence on domain wall sea), the energy of the $q\bar{q}$ component is derived at different valence quark masses, and shows a linear dependence on m_π^2. The slope is determined to be $c_1=0.505(3)\text{GeV}^{-1}$, from which the valence πρ sigma term is extracted to be $\sigma_{\pi\rho}^{(\text{val})}=9.82(6)$ MeV using the Feynman-Hellman theorem. At the physical pion mass, the mass of the $q\bar{q}$ component is interpolated to be $m_\rho=775.9\pm6.0\pm1.8$ MeV, which is close to the ρ resonance mass. We also obtain the leptonic decay constant of the $q\bar{q}$ component to be $f_{\rho^-}=208.5\pm5.5\pm0.9$ MeV, which can be compared with the experimental value $f_\rho^{\text{exp}}\approx221$ MeV through the relation $f_\rho^{\text{exp}}=\sqrt{Z_\rho}f_{\rho^\pm}$, with $Z_\rho\approx1.13$ being the on-shell wavefunction renormalization of ρ owing to the ρ−π interaction. We emphasize that m_ρ and f_ρ of the $q\bar{q}$ component, which are obtained for the first time from QCD, can be taken as the input parameters of ρ in effective field theory studies where ρ acts as a fundamental degree of freedom.

Keywords: ρ resonance, leptonic decay constant, renormalization

PACS: 12.38.Gc, 13.20.Jf, 14.40.Be **DOI:** 10.1088/1674-1137/42/6/063102

1 Introduction

The vector meson ρ is a well-known hadron resonance which appears in the $I=1$ and $L=1$ ππ system with the resonance parameters $m_\rho=775$ MeV and $\Gamma_\rho=149$ MeV. On the other hand, ρ is assigned in the quark model to be the $I=1$ member of the $q\bar{q}$ vector meson nonet with mass around 1 GeV. The connection between the resonance ρ in experiments and the confined $q\bar{q}$ quark model ρ was established by Jaffe by introducing concepts such as *ordinary* and *extraordinary* hadrons [1]. In this picture, $q\bar{q}$ mesons, glueballs, and hybrids are *ordinary* mesons, which decay into multi-hadron final states through the creation of new quanta ($q\bar{q}$ pairs or gluons) and develop widths proportional to $1/N_c$. In the large N_c limit, ordinary mesons decouple and appear as bound states with discrete energies, such that the Hilbert space is composed of discretized bound states and multi-hadron continuum states. In contrast, *extraordinary* hadrons show up as resonances in hadron-hadron interactions but diminish at large N_c. As far as the ρ meson is concerned, there is a confined channel corresponding to the quark model ρ and its excited states, as well as an open channel of ππ scattering states. The coupling between both channels results in the ρ resonance of an $O(1/N_c)$ width. This argument coincides with the result of a chiral perturbation theory study of ρ [2] which shows that while the ρ mass keeps almost constant, the width decreases with increasing N_c. This implies that ρ is a well-defined confined $q\bar{q}$ state in the $N_c\to\infty$ limit.

Even though this picture cannot be tested experimentally, since $N_c=3$ in the real world and ρ usually shows up as a resonance, one can resort to the lattice QCD formalism for the related investigation. On the finite

Received 8 March 2018, Published online 27 April 2018

∗ Supported in part by the U.S. DOE Grant No. DE-SC0013065, the National Nature Science Foundation of China (NSFC) (11335001, 11575196, 11575197, 11621131001) (CRC110 by DFG and NSFC), A. A. is supported in part by the National Science Foundation CAREER (PHY-1151648) and by U.S. DOE (DE-FG02-95ER40907), Y. C. thanks the CAS Center for Excellence in Particle Physics (CCEPP) for their support, this research used the resources of the Oak Ridge Leadership Computing Facility at the Oak Ridge National Laboratory, which is supported by the Office of Science of the U.S. Department of Energy (DE-AC05-00OR22725)

1) E-mail: cheny@ihep.ac.cn

Euclidean space-time lattice, the eigenstates of the QCD Hamiltonian have a discrete spectrum. For the case of ρ, if there exists a Hilbert space expanded by both the non-interacting ππ states and confined $q\bar{q}$ states, the QCD eigenstates can be viewed as state vectors in this Hilbert space. The last decade witnessed extensive lattice QCD efforts on the ρ resonance from ππ scattering [3–10], where the use of the $q\bar{q}$ operator and ππ operators is required and the eigen energies are used to extract the resonance parameters of ρ using Lüscher's formalism [11]. In addition to the great success in this direction, it is also an interesting question whether the would-be confined $q\bar{q}$ ρ can be accessed directly through the full-QCD lattice calculation. The major consideration is that one can use an interpolation field operator which couples weakly to ππ states but which couples almost exclusively to $q\bar{q}$ confined states. We find that the Coulomb gauge fixed wall-source $q\bar{q}$ operator serves this goal. As such, we can obtain the mass of the ρ bound state and its decay constant, as well as the chiral behavior of these quantities. Phenomenologically, the properties of the confined $q\bar{q}$ state ρ may shed light on the intrinsic dynamics of the ρ resonance. This strategy can be potentially extended to the study of other resonances, such as the Δ baryon, K^* resonance, and so on.

This paper is organized as follows. Section 2 presents the derivation of the m_π dependence of the confined $q\bar{q}$ ρ mass and the relevant discussion. Section 3 is devoted to the extraction of the leptonic decay constant of ρ. The conclusions and a summary can be found in Section 4.

2 ρ meson mass

Gauge configurations of $N_{\rm f} = 2+1$ domain-wall fermions with large spatial volume and physical pion mass have been generated by the RBC & UKQCD Collaborations [12]. This work is based on the 48I gauge ensemble with lattice size $L^3\times T=48^3\times 96$ [12]. The lattice spacing has been determined to be $a^{-1}=1.730(4)$ GeV, such that the spatial extension of the lattice is approximately $La\sim 5.5$ fm. The light sea quark mass is set to give the pion mass $m_\pi^{(\rm sea)} = 139.2(4)$ MeV. For the valence quarks, we adopt the overlap fermion action, which is another realization of chiral fermions on the lattice. The low-energy constant $\Delta_{\rm mix}$, which measures the mismatch of the mixed valence and sea pion masses between the domain-wall fermion and the overlap fermion, is shown to be very small [13]. Since the overlap fermion accommodates the multi-mass algorithm and the eigenvectors are the same for different quark masses, we use 1000 pairs of eigenvectors plus the zero modes for deflation in calculating quark propagators for several masses on 45 configurations (see Ref. [14] for details). The bare mass parameters are chosen as $am_q^{(\rm val)} = 0.00170$,0.00240,0.00300,0.00455,0.00600 and 0.02030, which give a pion mass ranging from 114 to 371 MeV. In this way we can discern the chiral behaviors of the mass and the leptonic decay constant of the ρ meson.

We first extract the decay constant of the pion according to the partially conserved axial current relation

$$m_\pi^2 f_\pi=(m_{\rm u}+m_{\rm d})\langle 0|\bar{u}\gamma_5 d|\pi\rangle, \tag{1}$$

which is free of renormalization since the quark mass renormalization constant Z_m and the renormalization constant Z_P of the pseudoscalar density $\bar{u}\gamma_5 d$ satisfy the relation $Z_m Z_P=1$ for overlap fermions. We obtain the pion masses and π decay constants which are listed in Table 1. Through a linear interpolation in m_π^2 near the physical pion mass m_π=139.5 MeV, we get f_π=131.3(6) MeV, which agrees with the RBC & UKQCD result $f_\pi=131.1(3)$ MeV on the same lattice and their final theoretical prediction $f_\pi = 130.2(9)$ MeV [12]. RBC & UKQCD also calculate f_π on a larger lattice with a smaller lattice spacing, $a^{-1}=2.359(7)$ GeV, with a result $f_\pi=130.9(4)$ MeV. Their f_π's on the two lattices imply very small finite a artifacts. This comparison can be taken as a calibration of our formalism.

In the calculation of the two-point functions in the ρ channel, the quark propagators are generated by spatial wall-sources after the gauge configurations are fixed to the Coulomb gauge first. This corresponds to using the Coulomb gauge fixed wall-source operator for the charged ρ,

$$O_{V,i}^{(\rm w)}(t)=\sum_{\boldsymbol{y},\boldsymbol{z}}\bar{u}(\boldsymbol{y},t)\gamma_i d(\boldsymbol{z},t). \tag{2}$$

In principle, this operator couples to all the eigenstates of the lattice Hamiltonian, which can be taken as the linear superpositions of $\pi\pi(I=1)$ scattering states and the confined $q\bar{q}$ states.

Table 1. Pion masses m_π, pion decay constants f_π, and masses of ρ for different bare valence quark masses.

$am_q^{(\rm val)}$/MeV	m_π/MeV	f_π/MeV	m_ρ/MeV
0.00170	114(2)	130.3(9)	773(7)
0.00240	135(2)	131.0(9)	775(6)
0.00300	149(2)	131.6(8)	779(6)
0.00455	182(2)	...	784(5)
0.00600	208(2)	...	789(5)
0.02030	371(1)	...	836(3)

For the sink operators of the vector, we use the spatially extended operators $O_{V,i}(\boldsymbol{x},t;\boldsymbol{r})$ by splitting the quark and antiquark field operators with different spatial displacements $\boldsymbol{r}$, namely, $O_{V,i}(\boldsymbol{x},t;\boldsymbol{r})=\bar{u}(\boldsymbol{x},t)\gamma_i d(\boldsymbol{x}+\boldsymbol{r},t)$. Subsequently, the two-point functions $C(t,r)$ with differ-

ent spatial separation r are calculated as

$$C(r,t)=\frac{1}{3N_r}\sum_{\boldsymbol{x},i,|\boldsymbol{r}|=r}\langle 0|O_{V,i}(\boldsymbol{x},t;\boldsymbol{r})O^{(\mathrm{w})\dagger}_{V,i}(0)|0\rangle, \qquad (3)$$

where N_r is the number of $\boldsymbol{r}$'s that satisfy $|\boldsymbol{r}|=r$.

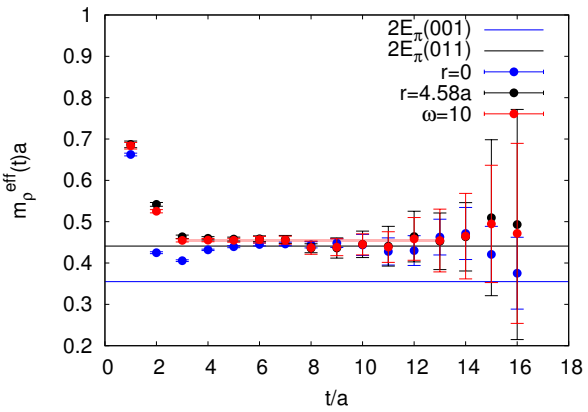

Fig. 1. (color online) The effective mass plateaus of ρ at $m_\pi = 208(2)$ MeV. The blue and black points are from the correlation functions $C(r=0,t)$ and $C(r=4.58a,t)$, respectively. The red points are from the mixed correlation function $C_{\mathrm{mix}}(t)=C(0,t)+\omega C(4.58a,t)$ with the mixing parameter $\omega=10$. The red band shows the fitted mass in the time range $t/a\in[3,13]$. The blue line and the black line are the energies of two non-interacting pions $2E_\pi$ with the momentum modes $\boldsymbol{p}a=2\pi/L(0,0,\pm1)$ and $\boldsymbol{p}a=2\pi/L(0,\pm1,\pm1)$, respectively.

The effective mass plateaus of $C(r,t)$ with $r=0$ (blue points) and $r=\sqrt{20}a=4.58a$ (black points) at $m_\pi=208(2)$ MeV are plotted in Fig. 1. It is seen that the plateaus lie on top of each other in the large-time range. The difference of the plateaus in the short-time range shows the r-dependence of the contamination from higher states. In order to reduce the excited-state contamination, we linearly combine the two correlation functions as $C_{\mathrm{mix}}(t)=C(0,t)+\omega C(4.58a,t)$ with an optimal mixing parameter $\omega\approx10$, by which we can get a very flat effective mass plateau starting from $t/a=3$, as shown in the figure (red points). We fit $C_{\mathrm{mix}}(t)$ using a single-exponential form in the time range $t/a\in[3,13]$ and get $m_V a=0.456(4)$ (plotted as a red band), where the error is statistical and is obtained through a jackknife analysis. We also plot the two lowest ππ P-wave thresholds $2E_\pi(001)=614$ MeV (shown in Fig. 1 as a blue line) and $2E_\pi(011)=761$ MeV (shown in Fig. 1 as a black line) with the relative momenta $\boldsymbol{p}a=2\pi/L(0,0,\pm1)$ and $\boldsymbol{p}a=2\pi/L(0,\pm1,\pm1)$, respectively. Since $2E_\pi(001)$ is far from the expected ρ mass, the corresponding ππ state should mix little with ρ and therefore have an energy close to $2E_\pi(001)$, but we do not observe this state.

The disappearance of the ππ states can be tentatively understood as follows. The wall-source operator $O^{(\mathrm{w})}_{V,i}(t)$ can be re-expressed as

$$O^{(\mathrm{w})}_{V,i}(t)=\sum_{\boldsymbol{y},\boldsymbol{z}}\bar{u}(\boldsymbol{y},t)\gamma_i d(\boldsymbol{z},t)\equiv\bar{\hat{u}}(\boldsymbol{0},t)\gamma_i\hat{d}(\boldsymbol{0},t), \qquad (4)$$

where $\hat{u}(\boldsymbol{0},t)$ and $\hat{d}(\boldsymbol{0},t)$ are the Fourier transformed quark fields in the momentum space with the spatial momentum $\boldsymbol{q}=\boldsymbol{0}$. Qualitatively in the picture of the non-relativistic constituent quark model, the matrix element $\langle 0|\bar{\hat{u}}(\boldsymbol{0},t)\gamma_i\hat{d}(\boldsymbol{0},t)|\rho^-\rangle$ can be interpreted as the probability amplitude of annihilating a zero-momentum anti-u quark and a zero-momentum d quark in the ρ^- state. If the ρ^- is at rest, then the average momenta of the constituent quarks are zero. Thus there is no suppression for this matrix element. However, for a P-wave $\pi^-\pi^0$ scattering state, the two pions must have non-zero relative momentum. In the center-of-mass frame of the two pions, let the momenta of π^- and π^0 be $\boldsymbol{p}$ and $-\boldsymbol{p}$, respectively. Then the average momenta of the anti-u quark in π^- and the d quark in π^0 are necessarily non-zero. Therefore the matrix element $\langle 0|\bar{\hat{u}}(\boldsymbol{0},t)\gamma_i\hat{d}(\boldsymbol{0},t)|\pi^-\pi^0\rangle$ will be strongly suppressed. On the other hand, we assume the $q\bar{q}$ confined states and the non-interacting ππ states establish a complete state basis for the Hilbert space when the ρ−ππ coupling is switched off. After inserting these states, the correlation function Eq. (3) can be expressed as

$$C(r,t)=\frac{1}{3N_r}\sum_{i,|\boldsymbol{r}|=r}\Bigg[\langle 0|O_{V,i}(\boldsymbol{0},t;\boldsymbol{r})|\rho^-\rangle\frac{1}{2m_{\rho^-}V}\langle\rho^-|O^{(\mathrm{w})\dagger}_{V,i}(0)|0\rangle$$
$$+\sum_{\boldsymbol{p}}\langle 0|O_{V,i}(\boldsymbol{0},t;\boldsymbol{r})|\pi^-(\boldsymbol{p})\pi^0(-\boldsymbol{p})\rangle\left(\frac{1}{2E_\pi(\boldsymbol{p})V}\right)^2\langle\pi^-(\boldsymbol{p})\pi^0(-\boldsymbol{p})|O^{(\mathrm{w})\dagger}_{V,i}(0)|0\rangle+\ldots\Bigg], \qquad (5)$$

where $V=L^3a^3$ is the spatial volume of the lattice, $1/(2m_{\rho^-}V)$ comes from the nomalization of $|\rho^-\rangle$, and $(1/(2E_\pi(\boldsymbol{p})V))^2$ comes from the ππ state $|\pi^-(\boldsymbol{p})\pi^0(-\boldsymbol{p})\rangle$. So the contribution of ππ states has an additional $1/L^3$ suppression factor.

This discussion also applies to the ππ state near the threshold $2E_\pi(011)=761$ MeV. So we argue that the plateau comes predominantly from the would-be $q\bar{q}$ confined state instead of the corresponding scattering state. In order to understand this theoretically, let us

consider a two-state system composed of the $q\bar{q}$ confined state $|\rho\rangle$ and the non-interacting $\pi\pi$ state $|\pi\pi\rangle$ with $H_0|\pi\pi\rangle = E_1|\pi\pi\rangle$, $H_0|\rho\rangle = E_2|\rho\rangle$, where H_0 is the Hamiltonian without coupling between ρ and $\pi\pi$. With the interaction of ρ and $\pi\pi$ included, the effective Hamiltonian can be written as the following 2×2 matrix in the representation space spanned by $|\rho\rangle$ and $|\pi\pi\rangle$, $H=H_0+H_{\rm I}=\begin{pmatrix} E_1 & x \\ x & E_2 \end{pmatrix}$. Upon introducing the parameters $M=\frac{1}{2}(E_1+E_2)$ (we assume $E_2>E_1$), $\Delta=E_2-E_1$, and $\delta=\sqrt{1+4x^2/\Delta^2}$, the eigenvalues of H are $E_\pm=M\pm\frac{1}{2}\Delta\delta$, which satisfy $H|\alpha_\pm\rangle=E_\pm|\alpha_\pm\rangle$ with $|\alpha_\pm\rangle=a_\pm|\pi\pi\rangle+b_\pm|\rho\rangle$. The explicit expressions of $a_\pm$ and $b_\pm$ are

$$\begin{pmatrix} a_- & b_- \\ a_+ & b_+ \end{pmatrix}=\frac{1}{\sqrt{2\delta}}\begin{pmatrix} \sqrt{\delta+1} & -\sqrt{\delta-1} \\ \sqrt{\delta-1} & \sqrt{\delta+1} \end{pmatrix}. \tag{6}$$

Subsequently, the Coulomb wall-source two-point function (note that the state normalization factor $1/2E$ has been absorbed into the definition of $|\ldots\rangle$, since $\langle\ldots|\ldots\rangle=1$) can be expressed as

$$\begin{aligned} C(t) &= \langle O_P(t)O_W^+(0)\rangle \\ &= \langle 0|O_P|\alpha_-\rangle\langle\alpha_-|O_W^+|0\rangle {\rm e}^{-E_-t} \\ &\quad +\langle 0|O_P|\alpha_+\rangle\langle\alpha_+|O_W^+|0\rangle {\rm e}^{-E_+t}. \end{aligned} \tag{7}$$

Applying the relation $\langle 0|O_W|\pi\pi\rangle=0$ and defining $Z_P=\langle 0|O_P|\rho\rangle$ and $Z_W=\langle 0|O_W|\rho\rangle$, the above equation can be rewritten as

$$\begin{aligned} C(t) &= Z_PZ_W(b_-^2{\rm e}^{-E_-t}+b_+^2{\rm e}^{-E_+t}) \\ &= Z_PZ_W{\rm e}^{-(M+\frac{1}{2}\Delta)t}\left[1+\frac{1}{2}x^2t^2(1+O(\Delta t))\right], \end{aligned} \tag{8}$$

where $M+\frac{1}{2}\Delta=E_2$ is exactly the mass of the $q\bar{q}$ confined state ρ ($H_0|\rho\rangle=E_2|\rho\rangle$) as defined before. One can also estimate x as follows [15]. According to Fermi's Golden Rule, the partial decay width of $\rho\to\pi\pi$ is expressed as $\Gamma=2\pi\langle x^2\rangle\rho(E)$ (note that $x=\langle\rho|H_I|\pi\pi\rangle$), where the angle bracket means the average over the spatial angle with $\langle x^2\rangle=x^2/3$, and $\rho(E)=L^3kE/(16\pi^2)$ is the spectral density. Thus we have $\Gamma=x^2L^3kE/(24\pi)$, which gives an estimate $ax\sim0.025$ using the physical width $\Gamma_\rho\sim150$ MeV and $a^{-1}=1.73$ GeV. If one uses the single-exponential function to fit the correlation function, the contribution of the x^2 term will give roughly $\leq1\%$ relative deviation from E_2, which is much smaller than the statistical errors and negligible. Thus we have argued that the plateau corresponds to the mass of the $q\bar{q}$ confined state ρ

$$C(t)\approx Z_PZ_W{\rm e}^{-E_2t}. \tag{9}$$

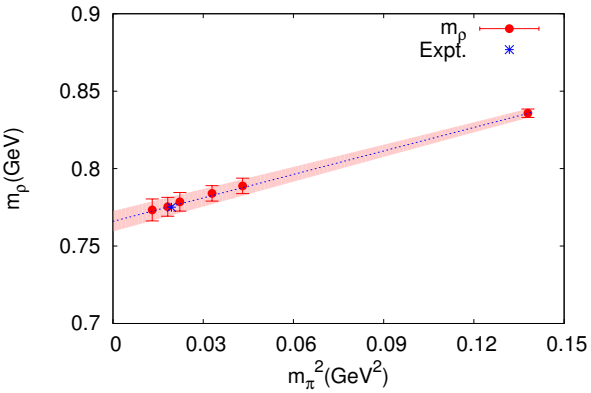

Fig. 2. (color online) The ρ mass $m_\rho=775.9\pm6.0$ MeV at the physical point is interpolated by $m_\rho(m_\pi)=m_\rho(0)+c_1m_\pi^2$ [16]. The red band shows the error of the interpolation. For comparison, the experimental value of $m_\rho=775$ MeV is plotted as the blue cross.

We follow a similar analysis procedure for the correlation functions at other pion masses. The extracted masses of ρ are listed in Table 1 and are also plotted in Fig. 2 with respect to m_π^2, by which the chiral behavior of m_ρ can be investigated. From Fig. 2 it is seen that m_ρ is very linear in m_π^2 for m_π ranging from 114 MeV to 371 MeV. A correlated jackknife analysis using the form [16]

$$m_\rho(m_\pi)=m_\rho(0)+c_1m_\pi^2, \tag{10}$$

gives $m_\rho(0)=766(7)$ MeV and $c_1=0.505(3)\,{\rm GeV}^{-1}$ with $\chi^2/d.o.f=0.13$. The ρ mass at the physical m_π is $m_\rho=775.9\pm6.0\pm1.8$ MeV, where the second error is due to the 0.23% uncertainty of the lattice spacing. Our data cannot discern higher order terms in m_π. We would like to point out that our study is the first to be carried out in the chiral region around the physical point and with chiral fermions, although there have been many lattice studies on this topic [17–20]. We note that c_1 is precisely determined, and potentially serves as a constraint on the chiral perturbation study of ρ. Furthermore, c_1 is exactly the valence or connected insertion part of the $\pi\rho$ sigma term from the Feynman-Hellman theorem $\sigma_{\pi\rho}^{\rm (val)}=m_\pi^2{\rm d}m_\rho/{\rm d}m_\pi^2=c_1m_\pi^2$, since the sea is fixed in our partially quenched calculation of m_ρ. From the fitted c_1 in Eq. (10), we find $\sigma_{\pi\rho}^{\rm (val)}=9.82(6)$ MeV. One can determine the disconnected part from a direct calculation of the $m\bar{\psi}\psi$ matrix element in the disconnected three-point correlator.

3 Leptonic decay constant of the ρ meson

The calculation of the decay constant of the charged ρ is straightforward [15, 21–25]. For the charged ρ, for

example, ρ^-, f_{ρ^-} is defined by

$$\langle 0|J_\mu^{(-)}(0)|\rho^-(\vec{p},\zeta)\rangle = m_\rho f_{\rho^-}\epsilon_\mu(\vec{p},\zeta), \tag{11}$$

where $J_\mu^{(-)}(x)=(\bar{u}\gamma_\mu d)(x)$ is the charged vector current and $\epsilon_\mu(\vec{p},\zeta)$ is the ζ-th polarization vector of ρ^- with $\zeta=1,2,3$. The spatial components of $J_\mu^{(-)}(x)$ are actually the operators $O_{V,i}(x;\boldsymbol{r}=0)$; therefore, the matrix element defined in Eq. (11) can be extracted from $C(r=0,t)$. The key challenge is to divide out the matrix element of the wall source operator $\langle 0|O_{V,i}^{(\mathrm{w})}|V(\vec{p},\zeta)\rangle$. Usually this matrix element can be derived by calculating the wall-wall correlation function

$$\begin{aligned} C^{(\mathrm{w})}(t) &\equiv \sum_r N_r C(r,t) = \frac{1}{3}\sum_i \langle 0|O_{V,i}^{(\mathrm{w})}(t)O_{V,i}^{(\mathrm{w}),\dagger}(0)|0\rangle \\ &= \frac{1}{3}\sum_{\boldsymbol{x},\boldsymbol{r},i}\langle 0|O_{V,i}(\boldsymbol{x},t;\boldsymbol{r})O_{V,i}^{(\mathrm{w}),\dagger}(0)|0\rangle, \end{aligned} \tag{12}$$

where the last equation uses the definition of $C(r,t)$ in Eq. (3).

However, very large statistics are required to obtain a satisfactory signal-to-noise ratio for this kind of correlation function. The reason for noisy $C^{(\mathrm{w})}(t)$ is explained as follows. Using the spectral expression $C(r,t)=\sum_i \Phi_n(r)\mathrm{e}^{-E_n t}$, when $t\to\infty$ one has

$$C^{(\mathrm{w})}(t) \approx \sum_r N_r \Phi_1(r)\mathrm{e}^{-E_1 t}. \tag{13}$$

In practice, we calculate $C(r,t)$ for r ranging from 0 to $10a$ and observe the profile of $\Phi_1(r)$ for $t=7a$ where all $C(r,t)$ are almost saturated by the ground state. The $\Phi_1(r)$ at $m_\pi=208(2)$ MeV (normalized as $\Phi_1(0)=1$) is plotted in Fig. 3 as red points. It is seen that $\Phi_1(r)$ damps rapidly with r and can be parameterized as

$$\Phi_1(r)=\Phi_1(0)\mathrm{e}^{-\left(\frac{r}{r_0}\right)^b}, \tag{14}$$

with the parameters $b=1.60$ and $r_0=5.88a$. The curve illustrates this parameterization in the figure.

We have checked this at other pion masses and find $\Phi_1(r)$ is similar for all the cases and is very insensitive to m_π. This means that when calculating the wall-to-wall correlation function $C^{(\mathrm{w})}(t)$, the $C(r,t)$'s (see Eq. (12)) with very large r contribute only noise and make $C^{(\mathrm{w})}(t)$ very noisy. In order to circumvent this difficulty, we introduce a cutoff r_c to exclude the contributions of $C(r,t)$'s with $r>r_\mathrm{c}$ from $C^{(\mathrm{w})}(t)$, and use the correlation function [26]

$$C^{(\mathrm{w})}(r_\mathrm{c},t)=\sum_{r\le r_\mathrm{c}} N_r C(r,t), \tag{15}$$

to approximate $C^{(\mathrm{w})}(t)$. Letting $I_1(r')=\int_0^{r'} dr r^2\Phi_1(r)$, one can see that the ratio $C^{(\mathrm{w})}(r_\mathrm{c},t)/C^{(\mathrm{w})}(t)$ can be depicted by the ratio $I_1(r_\mathrm{c})/I_1(\infty)$ at large t. The ratio $I_1(r_\mathrm{c})/I_1(\infty)$ using the parameterization above is also plotted in Fig. 3. It approaches 1 beyond $r_\mathrm{c}=15a$ and is equal to 0.995 at $r_\mathrm{c}=20a$, whose deviation from 1 is already much smaller than the statistical error. So we take $C^{(\mathrm{w})}(20a,t)$ as a satisfactory approximation of $C^{(\mathrm{w})}$ throughout this work.

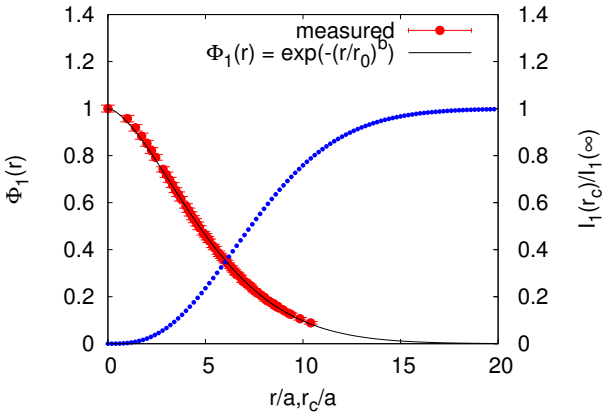

Fig. 3. (color online) The red points show $\Phi_i(r)$, showing a fall-off of $C(r,t)$ when r increases. The parameterization of $\Phi_1(r)$ is plotted by the curve. The blue points are the ratios $I_1(r_\mathrm{c})/I(\infty)$ at different r_c.

Using these parameters, the theoretical ratio $C^{(\mathrm{w})}(r_\mathrm{c},t)/C^{(\mathrm{w})}(t)$ deviates from 1 by roughly 0.5% at $r_\mathrm{c}=20a$ in the time range where the ground state dominates, which is much smaller that the relative error of $C^{(\mathrm{w})}(r_\mathrm{c},t)$. So we take $r_\mathrm{c}=20a$ in practice. With this prescription, we jointly fit the following functions to extract the decay constant,

$$\begin{aligned} C(0,t) &= \sum_n 2m_n L^3 f_n Z_n^{(\mathrm{w})}\mathrm{e}^{-m_n t}, \\ C^{(\mathrm{w})}(20a,t) &\approx \sum_n 2m_n L^3 (Z_n^{(\mathrm{w})})^2\mathrm{e}^{-m_n t}, \end{aligned} \tag{16}$$

where $Z_n^{(\mathrm{w})}$ is the matrix element of the wall source operator between the vacuum and the n-th state, and f_n is the decay constant of the n-th state according to the definition in Eq. (11). In practice, two exponentials are used in the fit and f_1 is taken as the bare decay constant of ρ. (The second term is introduced to account for the contamination of higher states.) Since f_1 is sensitive to the value of m_1, we adopt the single-elimination jackknife analysis procedure as follows. On each jackknife re-sampled ensemble, we first obtain the mass parameter m_1 from $C_{\mathrm{mix}}(t)$ defined previously, and then extract f_1 through a joint fit to Eq. (16) with m_1 fixed. After that, we quote the jackknife error of f_1 as the statistical error.

In calculating the renormalization constant Z_V of the vector current, we use the relation $Z_V=Z_A$ (Z_A is the renormalization constant of the axial vector current)

since the overlap fermions obey exact chiral symmetry on the lattice. Following the non-perturbative renormalization procedure in Ref. [27], we calculate Z_A from the Ward identity for a few bare quark masses, which gives $Z_A = 1.1045(8)$ in the chiral limit. Z_A and the renormalized decay constant f_ρ at different m_π are listed in Table 2. Figure 4 shows the chiral behavior of f_ρ, from which we get

$$f_{\rho^\pm} = 208.5 \pm 5.5 \pm 0.9 \text{ MeV} \quad (17)$$

through a linear interpolation in m_π^2 in the neighborhood of the physical pion mass, or specifically, in the range $m_\pi^2 \in [0.012, 0.044]\,\text{GeV}^2$. We do not include the result at $m_\pi = 0.371$ GeV for the interpolation since the linear fit in m_π^2 is invalid at this m_π. The first error is statistical and the second is the combined uncertainty of Z_V, the scale parameter a^{-1}, and the approximated wall-wall correlation function.

Table 2. The renormalization constant Z_A obtained at different pion masses, which also gives Z_V by the relation $Z_A = Z_V$ for overlap fermions. The renormalized decay constants f_ρ are also listed.

m_π/MeV	Z_A	f_ρ/MeV
114(2)	1.103(4)	206(7)
135(2)	1.103(3)	208(7)
149(2)	1.104(2)	211(6)
182(2)	1.104(2)	215(5)
208(2)	1.105(1)	217(5)
371(1)	1.105(1)	223(3)

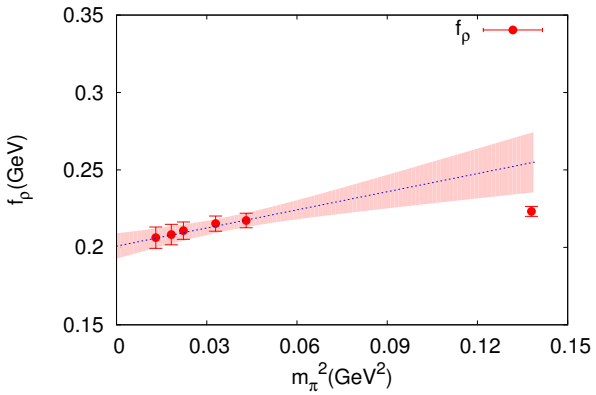

Fig. 4. (color online) The decay constant f_ρ obtained at different pion masses. The curve shows the linear interpolation in terms of m_π^2.

In τ decays, the branching fraction of the process $\tau \to \rho^- \nu_\tau$ is $\mathcal{B}_\rho = 25.21(33)\%$, which results from subtracting the 0.31(32)% non-$\rho(770)$ contribution from the $\tau \to \pi^-\pi^0\nu_\tau$ branching fraction 25.52(9)% [28]. $\mathcal{B}_\rho$ gives $f_{\rho^-}^{\rm exp} = 221.1 \pm 1.6$ MeV when Γ_ρ is taken into account. On the other hand, the partial decay width $\Gamma(\rho^0 \to e^+e^-) = 7.04(6)$ keV [28] gives $f_{\rho^0}^{\rm exp} = 221(1)$ MeV if one takes the quark-model value $\bar{Q}_{\rho^0}^2 = 1/2$ of ρ^0 effective charge squared. $f_{\rho^0}^{\rm exp} \approx f_{\rho^\pm}^{\rm exp}$ is the natural result of the conservation of the vector current (CVC). The experimental values deviate from our prediction by roughly 6%. This discrepancy can be understood as follows. If the $q\bar{q}$ confined state ρ we have obtained is viewed as the free (bare) ρ state, f_ρ is actually the transition amplitude of the free ρ to a gauge boson ($W^\pm$ for charged ρ and photon for the neutral ρ). When the $\rho-\pi$ interaction is switched on, according to the LSZ reduction formula, the amplitude $f_\rho^{\rm exp}$ of the physical ρ is related to f_ρ by $f_\rho^{\rm exp} = \sqrt{Z_\rho} f_\rho$ with $Z_\rho \approx 1.13$ [29] the on-shell wave function renormalization coming from the ρ self-energy. In other words, the 6% deviation from $f_\rho^{\rm exp}$ is exactly described by $\sqrt{Z_\rho} \approx 1.06$.

4 Conclusion

To summarize, we argue that the $q\bar{q}$ wall source operator in a fixed gauge can strongly suppress P-wave scattering states such that the $q\bar{q}$ component of an ordinary meson, such as ρ, can be accessed in a lattice QCD study. For the case of ρ, this $q\bar{q}$ component can be taken as the bare $q\bar{q}$ confined state with a mass of $m_\rho = 775.9 \pm 6.0 \pm 1.8$ MeV at the physical pion mass, which is almost the same as the pole mass of the ρ resonance. This observation reinforces the chiral perturbation theory study and the so-called *ordinary meson* argument of the ρ resonance that the $\rho-\pi$ interaction does not shift the mass of ρ much but contributes to its width. m_ρ is almost linear in m_π^2 and the slope $c_1 = 0.505(3)\,\text{GeV}^{-1}$ also gives the valence $\pi\rho$ sigma term, which gives $\sigma_{\pi\rho}^{(\rm val)} = 9.82(6)$ MeV from the Feynman-Hellman theorem. We also extract the leptonic decay constant of the bare $\rho^\pm$ state to be $f_{\rho^\pm} = 208.5 \pm 5.5 \pm 0.9$ MeV at the physical m_π, whose deviation from the experimental value $f_\rho^{\rm exp} \approx 221$ MeV is explained by $f_\rho^{\rm exp} = f_{\rho^\pm}\sqrt{Z_\rho}$ with $Z_\rho \approx 1.13$ being the on-shell wavefunction renormalization of ρ owing to the $\rho-\pi$ interaction. This study may shed new light on the nature of the ρ resonance and also be helpful to understand the properties of other hadron resonances.

We are very grateful for valuable discussions with Prof. Q. Zhao and Prof. K.-F. Liu. We thank the RBC & UKQCD Collaborations for providing us with their DWF gauge configurations.

References

1 R. L. Jaffe, AIP Conf. Proc., **964**: 1 (2007); Prog. Theor. Phys. Suppl., **168**: 127 (2007) [arXiv:hep-ph/0701038]
2 J. R. Pelaez, Phys. Rev. Lett., **92**: 102001 (2004) [arXiv:hep-ph/0309292]
3 X. Feng, K. Jansen, and D. B. Renner, Phys. Rev. D, **83**: 094505 (2011) [arXiv:1011.5288(hep-lat)]
4 C. Pelissier and A. Alexandru, Phys. Rev. D, **87**: 014503 (2013) [arXiv:1211.0092 (hep-lat)]
5 S. Aoki et al (PACS-CS Collaboration), Phys. Rev. D, **84**: 094505 (2011) [arXiv:1106.5365 (hep-lat)]
6 J. J. Dudek, R. G. Edwards, and C. E. Thomas (Hadron Spectrum Collaboration), Phys. Rev. D, **87**: 034505 (2013); Phys. Rev. D, **90**: 099902(E) (2014) [arXiv:1212.0830 (hep-ph)]
7 G. Bali et al (RQCD Collaboration), Phys. Rev. D, **93**: 054509 (2016) [arXiv:1512.08678 (hep-lat)]
8 D. Guo, A. Alexandru, and R. Molina, Phys. Rev. D, **94**: 034501 (2016) [arXiv:1605:03993 (hep-lat)]
9 Z. Fu and L. Wang, Phys. Rev. D, **94**: 034505 (2016) [arXiv:1608.07478 (hep-lat)]
10 J. Bulava, B. Fahy, B. Hörz, K. J. Juge, C. Morningstar, and C.H. Wong, Nucl. Phys. B, **910**: 842 (2016) [arXiv:1604.05593 (hep-lat)]
11 M. Lüscher, Commun. Math. Phys., **105**: 153 (1986)
12 T. Blum et al (RBC and UKQCD Collaborations), Phys. Rev. D, **93**: 074505 (2016) [arXiv:1411.7017 (hep-lat)]
13 M. Lujan, A. Alexandru, Y. Chen, T. Draper, W. Freeman, M. Gong, F. X. Lee, A. Li, K.-F. Liu, and N. Mathur, Phys. Rev. D, **86**: 014501 (2012) [arXiv:1204.6256 (hep-lat)]
14 A. Alexandru, M. Lujan, C. Pelissier, B. Gamari and F. X. Lee, arXiv:1106.4964 (hep-lat)
15 C. McNeile and C. Michael (UKQCD Collaboration), Phys. Lett. B, **556**: 177(2003) [arXiv:hep-lat/0212020]
16 P. C. Bruns and U.-G. Meissner, Eur. Phys. J. C, **40**: 97 (2005)
17 C. W. Bernard et al, Phys. Rev. D, **64**: 054506 (2001) [arXiv: hep-lat/0104002]
18 D. B. Leinweber, A. W. Thomas, K. Tsushima, and S. V. Wright, Phys. Rev. D, **64**: 094502 (2001) [arXiv: hep-lat/0104013]
19 C. R. Allton, W. Armour, D. B. Leinweber, A. W. Thomas, and R. D. Young, Phys. Lett. B, **628**: 125 (2005) [arXiv: hep-lat/0504022]
20 W. Armour, C. R. Allton, D. B. Leinweber, A. W. Thomas, and R. D. Young, J. Phys. G, **32**: 971 (2006) [arXiv: hep-lat/0510078]
21 R. Lewis and R. M. Woloshyn, Phys. Rev. D, **56**: 1571 (1997) [arXiv: hep-lat/9610027]
22 A. Ali Khan et al (CP-PACS Collaboration), Phys. Rev. D, **65**: 054505 (2002) [arXiv: hep-lat/0105015]
23 M. Gockeler, R. Horsley, D. Pleiter, P.E.L. Rakow, G. Schierholz, W. Schroers, H. Stüben, and J.M. Zanotti, Proc. Sci. LAT, **2005**: 063 (2006) [arXiv: hep-lat/0509196]
24 K. Hashimoto and T. Izubuchi, Prog. Theor. Phys., **119**: 599 (2008) [arXiv:0803.0186 (hep-lat)]
25 K. Jansen, C. McNeile, C. Michael, and C. Urbach (ETM Collaboration), Phys. Rev. D, **80**: 054510 (2009) [arXiv:0906.4720 (hep-lat)]
26 K. F. Liu, J. Liang, and Y. B. Yang, Phys. Rev. D, **97**: 034507 (2018) [arXiv:1705.06358 (hep-lat)]
27 Z. Liu, Y. Chen, S.-J. Dong, M. Glatzmaier, M. Gong, A. Li, K.-F. Liu, Y.-B. Yang, and J.-B. Zhang (χQCD Collaboration), Phys. Rev. D, **90**: 034505 (2014) [arXiv:1312.7628 (hep-lat)]
28 C. Patrignani et al (Particle Data Group), Chin. Phys. C, **40**: 100001 (2016)
29 F. Jegerlehner and R. Szafron, Eur. Phys. J. C, **71**: 1632 (2011) [arXiv:1101.2872 (hep-ph)]